Molecular Biology of the Cell
Vol. 17, 4720–4735, November 2006

A Coiled-Coil Domain of Melanophilin Is Essential for Myosin Va Recruitment and Melanosome Transport in Melanocytes[D]

Alistair N. Hume,* Abul K. Tarafder,* José S. Ramalho,† Elena V. Sviderskaya,‡ and Miguel C. Seabra*

*Molecular and Cellular Medicine, Division of Biomedical Sciences, Imperial College London, London SW7 2AZ, United Kingdom; †Centre of Ophthalmology, Biomedical Institute for Research in Light and Image, University of Coimbra, 3000 Coimbra, Portugal; and ‡Department of Basic Medical Sciences, St. George's, University of London, London SW17 0RE, United Kingdom

Submitted May 25, 2006; Accepted August 9, 2006
Monitoring Editor: Jennifer Lippincott-Schwartz

Melanophilin (Mlph) regulates retention of melanosomes at the peripheral actin cytoskeleton of melanocytes, a process essential for normal mammalian pigmentation. Mlph is proposed to be a modular protein binding the melanosome-associated protein Rab27a, Myosin Va (MyoVa), actin, and microtubule end-binding protein (EB1), via distinct N-terminal Rab27a-binding domain (R27BD), medial MyoVa-binding domain (MBD), and C-terminal actin-binding domain (ABD), respectively. We developed a novel melanosome transport assay using a Mlph-null cell line to study formation of the active Rab27a:Mlph:MyoVa complex. Recruitment of MyoVa to melanosomes correlated with rescue of melanosome transport and required intact R27BD together with MBD exon F–binding region (EFBD) and unexpectedly a potential coiled-coil forming sequence within ABD. In vitro binding studies indicate that the coiled-coil region enhances binding of MyoVa by Mlph MBD. Other regions of Mlph reported to interact with MyoVa globular tail, actin, or EB1 are not essential for melanosome transport rescue. The strict correlation between melanosomal MyoVa recruitment and rescue of melanosome distribution suggests that stable interaction with Mlph and MyoVa activation are nondissociable events. Our results highlight the importance of the coiled-coil region together with R27BD and EFBD regions of Mlph in the formation of the active melanosomal Rab27a-Mlph-MyoVa complex.

INTRODUCTION

Melanocytes produce melanin pigment in mammals and reside in the skin, eye, ear, meninges, and Harderian gland. Melanin is synthesized by sequential oxidation and hydroxylation of tyrosine and is stored in the cytoplasm in membrane-bound melanosomes (Ito, 2003). These organelles share some characteristics with lysosomes, e.g., acidic pH and the presence of some lysosomal resident proteins, but also have distinct components such as tyrosinase, TRP-1, and TRP-2, which are involved in melanogenesis (Marks and Seabra, 2001). Skin melanocytes reside in the basal layer of the epidermis and hair bulbs where their highly dendritic morphology allows them to contact and transfer pigment into many dividing keratinocytes.

Mouse and human genetic studies have identified a number of gene products involved in normal pigmentation (Bennett and Lamoreux, 2003). Many of these products are believed to contribute to the specialized membrane-trafficking events required for melanogenesis, and a subset has been identified that appears to affect the intracellular melanosome distribution and intercellular transport instead of biogenesis. These mouse mutants and patients are thought to suffer albinism as a result of the fact that pigment accumulates around the melanocyte nucleus and transfers in an abnormal manner from melanocyte dendrites to keratinocytes (Marks and Seabra, 2001). Seminal videomicroscopic studies of melanosome movements in melanocytes from one such mutant (*dilute*) that is defective in the molecular motor MyoVa indicated that melanosomes undertake microtubule-based transport to the dendrite tips and then are retained there by MyoVa-mediated interaction with the cortical actin cytoskeleton (Wu *et al.*, 1998). Functional loss of Rab27a, as in *ashen* mice and Griscelli Syndrome 2 (GS2), or Mlph (also known as Slac2-a), as in *leaden* mice and GS3, result in similar defects in intracellular transport of mature melanosomes implicating these three gene products in the same pathway. We and others have established that active GTP-bound Rab27a associates with melanosomes, resulting in the sequential recruitment of the modular adaptor protein Mlph and the actin-dependent motor MyoVa, resulting in coupling of melanosomes to the cortical actin cytoskeleton

This article was published online ahead of print in *MBC in Press* (http://www.molbiolcell.org/cgi/doi/10.1091/mbc.E06–05–0457) on August 16, 2006.

[D] The online version of this article contains supplemental material at *MBC Online* (http://www.molbiolcell.org).

Address correspondence to: Miguel C. Seabra (m.seabra@imperial.ac.uk).

Abbreviations used: ABD, actin-binding domain; EB1, end-binding protein 1; EFBD, exon F-binding domain; GS, Griscelli syndrome; GTBD, globular tail-binding domain; *ln*, leaden; MBD, myosinVa–binding domain; Mlph, melanophilin; R27BD, Rab27a-binding domain; SHD, synaptotagmin homology domain; ZnF, Zn^{2+} finger; TRP1, tyrosinase-related protein 1; TRP2, tyrosinase-related protein 2.

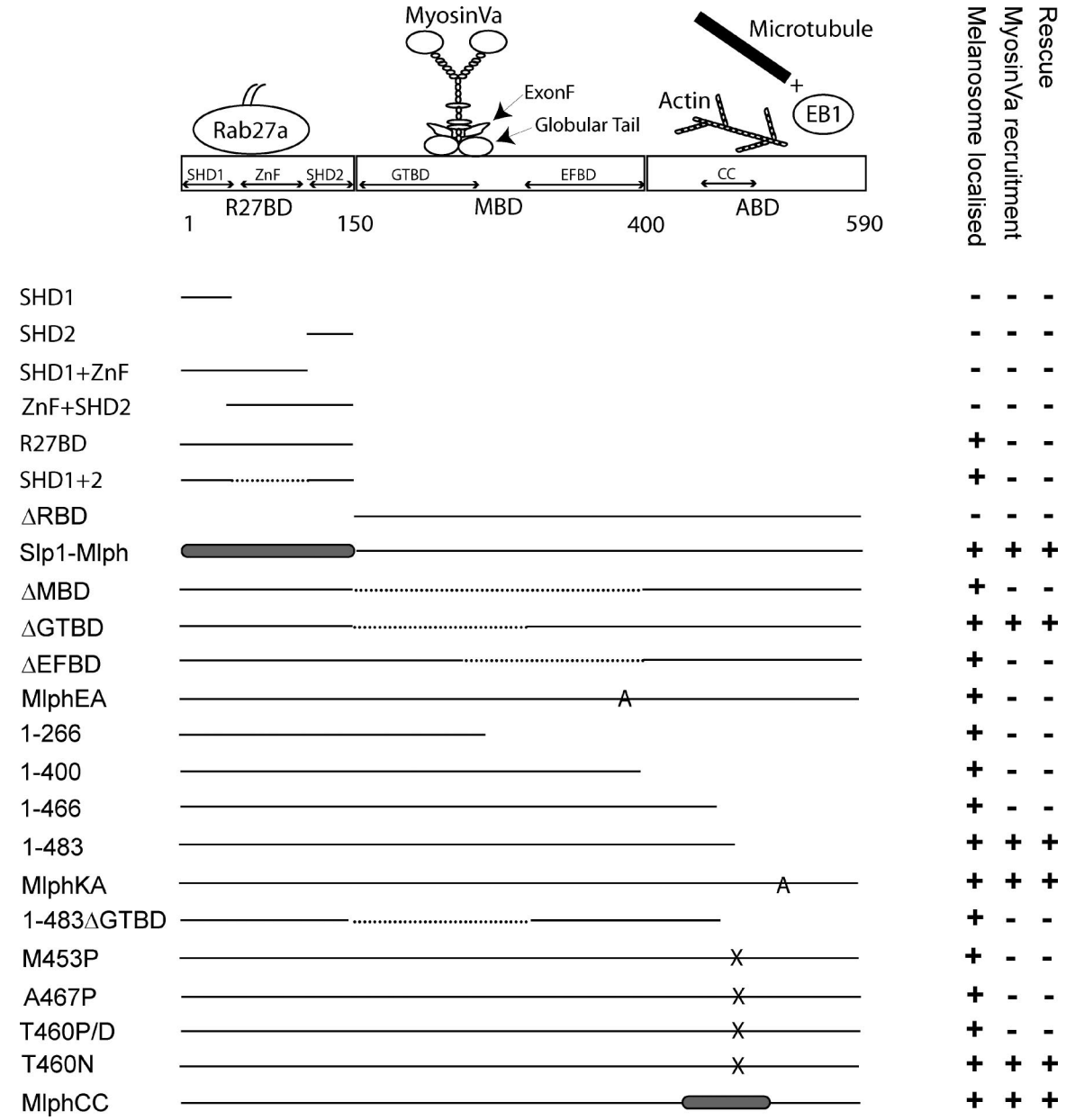

Figure 1. Summary of the functional characteristic of Mlph constructs used in this study. The top part of the figure is a schematic representation of the domain structure of Mlph showing the regions previously shown to be involved in interaction with other proteins. In the bottom part of the figure solid lines indicate wild-type Mlph sequence, dashed lines indicate internal truncations, gray shaded areas indicate non-Mlph sequence within chimeric proteins, and letters A and X indicate the position of ala or other substitutions in point mutants. Each construct is scored + or − for its ability to be recruited to melanosomes, the ability to recruit MyoVa to melanosome and its ability to rescue melanosome transport defects in melan-ln cells.

(Fukuda *et al.*, 2002; Nagashima *et al.*, 2002; Strom *et al.*, 2002; Wu *et al.*, 2002a).

Mlph is one of a growing family of Rab27a "effector" proteins, i.e., proteins that preferentially bind the activated GTP-bound form of Rab27a (Fukuda, 2005). There is some evidence that cell type–specific expression of this diverse effector family allows Rab27a to fulfill different functions in the different cell types in which it is expressed (Hume *et al.*, 2002). With the exception of Munc13-4, all these proteins contain an N-terminal 150 aa Rab27-binding domain (R27BD) comprising two SHD domains, which may be adjacent or separated by a putative Zn^{2+} finger motif (ZnF). In Slp1/JFC1, Slp2-a, Slp3-a, Slp4-a/granuphilin-a, Slp5, and Rabphilin, the R27BD is followed by tandem C2 domains, which mediate phospholipid binding, and there is evidence that these proteins, together with Noc2 and Munc13-4, regulate fusion of secretory granules with the plasma membrane in several cell types (Fukuda, 2005).

In contrast, Mlph/Slac2-a and MyRIP/Slac2-c have similar medial and C-terminal sequences that lack tandem C2 domains and play a role in binding members of the myosin family of molecular motors, MyoVa and MyoVa/VIIa, respectively, and actin (Fukuda and Kuroda, 2002). Consequently, these proteins are both thought to play a role in organelle movement rather than secretion. A number of

Table 1. The statistical significance of melanosome transport rescue data for each construct used in this study measured against positive and negative controls

Construct transfected	p value vs. Mlph	p value vs. Slp1
ΔMBD	0.0000	0.8171
ΔGTBD	0.2481	0.0000
ΔEFBD	0.0000	0.0028
EA	0.0000	0.8989
1-266	0.0000	0.7777
1-400	0.0000	0.8735
1-466	0.0000	0.3202
1-483	0.9054	0.0000
KA	0.5287	0.0000
1-483ΔGTBD	0.0000	0.9802
T460P	0.0000	0.6736
M453P	0.0000	0.2976
T460D	0.0000	0.7575
T460N	0.0428	0.000
C-C	0.0126	0.000

recent studies have investigated the role of the C-terminus of Mlph in melanosome transport and its role in binding MyoVa, actin, and EB1 (Figure 1). Our laboratory and others found the medial region of Mlph to be necessary and sufficient for binding of the C-terminal tail domain of MyoVa (aa 1258-1853 in mouse; Nagashima *et al.*, 2002; Strom *et al.*, 2002). Moreover, the melanocyte-specific exon F appears to be absolutely required for MyoVa to interact with Mlph (Wu *et al.*, 2002a). More recently it has been proposed that a second domain of interaction between the globular tail of MyoVa and a more N-terminal region (aa 147-240 of mouse sequence) Mlph may exist (Fukuda and Kuroda, 2002, 2004). It has also been suggested that the C-terminus of Mlph (mouse aa 400-590) may directly interact with actin and that this is important in allowing proper melanosome distribution to the dendrite tips (Kuroda *et al.*, 2003). Finally, the C-terminus of Mlph (aa 490-590 in mouse) has been implicated in binding EB1. This interaction might allow it to track to the peripheral dendrite tips on the plus-end tips of growing microtubules, where it would reside in complex with actin-associated MyoVa until a suitable Rab27a-associated melanosome could be captured (Wu *et al.*, 2005).

The primary objective of the present study was to examine the contribution of the individual domains of Mlph to its overall function. To achieve this end, we have established a novel cell culture melanosome transport assay that measures the extent of recovery of melanosome transport defects in *leaden* (*ln*) melanocytes, that result from overexpression of Mlph and mutants that specifically lack individual domains. This cell culture melanosome transport assay allowed us to examine questions arising from the genetic and biochemical data in a cellular context.

MATERIALS AND METHODS

Plasmids

Preparation of pEGFPC2-Mlph was described previously (Strom *et al.*, 2002). Plasmids pCS-26xMyc-Mlph SHD1, pCS-26xMyc-MlphSHD1+ ZnF, pCS-26xMyc-MlphSHD1+ ZnF +SHD2, pCS-26xMyc-Mlph ZnF +SHD2, pCS-26xMyc-MlphSHD2, pCS-26xMyc-MlphSHD1+SHD2, pCS-26xMyc-Mlph$^{1-266}$, pCS-26xMyc-Mlph$^{1-400}$, pCS26xMyc-Mlph$^{1-466}$, pCS26xMyc-Mlph$^{1-483}$, pCS26xMyc-Mlph$^{1-590}$, pCS26xMyc-Mlph$^{150-590}$, pCS-26xMyc-MlphΔMBD, pCS-26xMyc-MlphΔEFBD, and pCS-26xMyc-MlphΔGTBD encoding murine melanophilin were produced by PCR amplification using IMAGE clone 4862487 as a template. pCS-26xMyc-Slp1 encoding full-length murine Slp1, was produced by PCR amplification using IMAGE clone 5320346 as a template. In the above cases PCR products were digested using restriction endonucleases EcoRI and XhoI and ligated into plasmid pCS-2 (a kind gift of Vania Braga, Imperial College, London) prepared using the same enzymes. This vector allows the production of the Mlph and Slp1 proteins N-terminus tagged with six consecutive copies of the myc epitope (MEQKLISEEDL) in mammalian cells. Plasmids pCS26xMyc-Mlph^{M453P}, pCS26xMyc-Mlph^{T460P}, pCS26xMyc-Mlph^{T460D}, pCS26xMyc-Mlph^{T460N}, pCS26xMyc-Mlph^{A467P}, pCS26xMyc-Mlph$^{D378A\ E380A\ E381A}$ (MlphEA), and pCS26xMyc-Mlph$^{K493A\ R495A\ R496A\ K497A}$ (MlphKA), which encode point mutant murine Mlph were produced using the Quikchange PCR mutagenesis kit (Stratagene, La Jolla, CA) with pCS26xMyc-Mlph$^{1-590}$ as a template.

pCS26xMycSlp1R27BD-Mlph encoding a Slp1:Mlph chimera in which the R27BD of Mlph (aa 1-153 in mouse) was replaced with the corresponding region of Slp1 (aa 1-116 in mouse) was produced by PCR amplification of the R27BD of Slp1. The PCR product was digested with HindIII and ligated into pEGFPC2-Mlph, prepared using the same enzyme. The insert from a correctly oriented recombinant clone was then PCR amplified, digested using EcoRI and XhoI, and then ligated into pCS26xMyc, prepared using the same enzymes. pCS26xMyc-MlphCC encoding a Mlph:MyRIP chimera in which aa 433-511 were replaced by the corresponding region of MyRIP (aa 799-862) was produced by consecutive introduction of SpeI and SalI restriction sites at positions 1300 and 1533 of Mlph coding sequence using pCS26xMyc-Mlph$^{1-590}$ as a template to create pCS26xMyc-Mlph$^{433Spe1\ 511SalI}$. The corresponding region of rat MyRIP coding sequence (nucleotides 2097-2346) was then amplified by PCR using pGAD-C3-MyRIP as a template. The amplified fragment was digested using SpeI and SalI restriction endonucleases and ligated into pCS-26xMyc-Mlph$^{433Spe1\ 511SalI}$, prepared using the same enzymes.

For production of pGEX-4T1-Mlph constructs, which allow the synthesis of fragments of Mlph fused at the C-terminus of GST, the appropriate regions of Mlph coding sequence were amplified by PCR using IMAGE clone 4862487 as a template. PCR products were digested with restriction enzymes EcoRI and XhoI and ligated into empty pGEX-4T1 prepared using the same enzymes. A pGEX-4T1 clone encoding GST-Mlph150-500AP was produced in the same way using pCS26xMyc-Mlph^{A467P} as a template. pMAL-c2XMyoVa MSGTA encoding MyoVa MS-GTA (aa 1260-1853 and including alternatively spliced exons D and F and lacking exon B) fused to the C-terminus of *E. coli* maltose-binding protein (MBP) was produced by subcloning of MyoVaMS-GTA from pLEX MyoVaMSGTA (Strom *et al.*, 2002) using EcoRI and SalI restriction endonucleases into pMAL-c2X (New England Biolabs, Beverly, MA) prepared using the same enzymes. The fidelity of sequences of clones was confirmed by DNA sequencing. All oligonucleotide primers were synthesized and desalted by Sigma-Genosys (Cambridge, United Kingdom), and alignment of protein sequences was using ClustalW available at http://pbil.univ-lyon1.fr/. The sequence of all oligonucleotide primers used in this study are available on request.

Generation and Maintenance of Immortal melan-ln Melanocytes

To facilitate the generation of immortal melanocytes, C57BL/6J-*ln fz H54*/+ + *H54*, mice homozygous for *ln* were crossed with C57BL6/J mice carrying an *Ink4a-Arf* exon 2 deletion (Serrano *et al.*, 1996). These crosses were performed at Texas A&M University (College Station, TX) by Lynn Lamoreux. Four individual trunk skins of neonatal F2 *ln/ln* mice were used at St George's, University of London, for preparation of melanocyte cultures, as described previously (Sviderskaya *et al.*, 2002), yielding immortal lines melan-ln1, 2, 3, and 4. These were maintained in RPMI 1640 medium supplemented with 10% fetal calf serum, 2 mM glutamine, 100 U/ml penicillin G, and 100 mg/ml streptomycin (all from Invitrogen, Paisley, United Kingdom), 200 nM phorbol 12-myristate 13-acetate, 200 pM cholera toxin (both from Sigma-Aldrich, Poole, United Kingdom), at 37°C with 10% CO_2. Melanocytes for transfection and microinjection were seeded onto glass coverslips at the appropriate density, grown overnight and used the following day. Data presented in this article were obtained in experiment using the melan-ln3 cell line; however, similar results were obtained when experiments were repeated in other melan-ln cell lines and primary cultures of melanocytes derived from *ln/ln* mice.

Transfection and Microinjection of Melanocytes

melan-ln melanocytes grown on 13-mm-diameter round coverslips were transfected in Optimem serum-free medium (Invitrogen) with plasmid DNA using Fugene6 transfection reagent (Roche, Lewes, United Kingdom) using a ratio of 0.5 μg DNA:2 μl of Fugene6. DNA:Fugene6 complexes were removed from cells after 3 h and replaced with full medium. melan-ln3 melanocytes were microinjected with pEGFPC2-Mlph (0.01 mg/ml) using a microscope (Axiovert 135m; Zeiss, Thornwood, NY) attached to an Eppendorf Microinjection Unit (Microinjector model 5242; Micromanipulator model 5170; CO_2 Controller model 3700, and Heat Controller model 3700) and micropipettes. Micropipettes were prepared from borosilicate glass capillaries (0.69 mm internal diameter Harvard Apparatus, Edenbridge, Kent, United Kingdom) using a Flaming-Brown pipette puller (Model P-97 Sutter Instruments, Novato, CA). During microinjection, cells were maintained at 37°C in a humid-

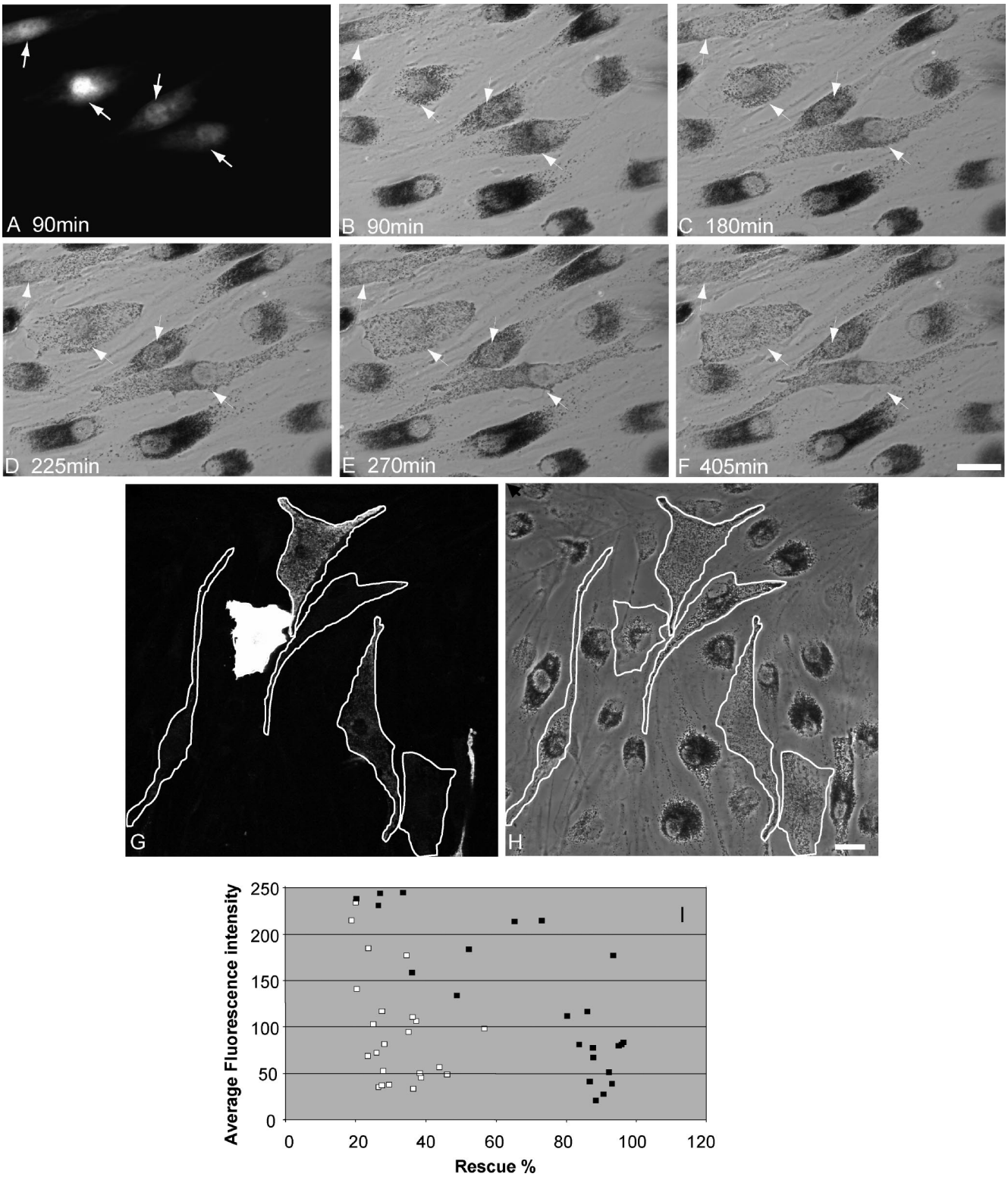

Figure 2. Melanosome transport defects in melan-ln cells may be rescued by the introduction of exogenous Mlph. (A–F) A time course of recovery of melanosome transport dynamics after exogenous expression of Mlph. Coverslip grown melan-ln melanocytes were coinjected with pEGFP-Mlph and Texas red dextran and melanosome distribution in injected cells was observed using phase-contrast optics. (A) The distribution of Texas red dextran and arrows indicate injected cells; (B–F) the position of melanosomes in the injected cells at the indicated time in minutes after injection. Panels G–I show that recovery of melanosome transport defects in melan-ln cells is sensitive to the level of expression of Mlph. Cells were transfected with plasmid encoding 6xmyc-Mlph, fixed 48 h later, stained using anti-myc antibodies, and observed by confocal microscopy. (G) A representative image of the distribution of overexpressed 6xmyc-Mlph in a number of melan-ln cells expressing varying levels of exogenous protein; (H) the distribution of melanosomes observed using transmission optics. White traces in G and H indicate that perimeter of transfected cells. (I) The relationship between Mlph expression level (average fluorescence intensity/pixel/cell)

ified 10% CO_2 atmosphere. To allow visualization of injected cells plasmid DNA was mixing with 5 mg/ml Texas red conjugated dextran (MW 10,000; Molecular Probes, Eugene, OR).

Immunofluorescence Microscopy

Coverslip-grown transfected cells were washed in PBS and then fixed in 3% paraformaldehyde in PBS for 15 min. Excess fixative was removed by washing in PBS and quenched by incubation in 50 mM NH_4Cl for 10 min. Fixed cells were then incubated with primary antibody diluted in solution 1 (PBS, 0.5% BSA, 0.05% saponin) for 30 min, washed extensively in solution 1 and incubated for 30 min with appropriate Alexa 488 and/or Alexa 568-conjugated secondary antibodies (Invitrogen) diluted 1:500 in solution 1. Coverslips containing fixed and stained cells were washed as before in solution 1, and mounted in ImmunoFluor medium (MP Biomedicals, Illkirch, France), and fluorescence and transmission images were captured using a Leica DM-IRBE confocal microscope (Deerfield, IL) fitted with 40× 1.0 NA oil-immersion FLUOTAR objective lens. Conditions for detection of MyoVa, myc-tagged proteins and Mlph have been described previously (Strom *et al.*, 2002). Images were processed using Leica TCS-NT software associated with the microscope and Adobe Photoshop CS software (San Jose, CA). All images presented are single sections in the *z*-plane. For quantitation of expression level and extent of rescue of melanosome transport, cells fixed and stained on the same day were examined blind the following day and nonsaturated 8-bit fluorescence and transmission images were obtained using identical laser power, PMT voltages, and acousto-optical filter settings. Using these images the total area, the melanosome-filled area and the average fluorescence intensity of cells was determined manually using NIH ImageJ software (http://rsb.inof.ni.gov/ij/). To determine the extent of rescue of melan-ln melanosome transport defects by introduced constructs, the rescue ratio was calculated by dividing the melanosome filled area by the total cell area. The statistical significance of results of the rescue assay for each experimental protein was determined by pairwise comparison of rescue ratios with those achieved by positive (Mlph) and negative (Slp1) control proteins using Student's *t* test (Table 1).

Time-Lapse Microscopy

Living melan-ln3 melanocytes expressing EGFP-Mlph were maintained at 37°C in growth medium in a closed FCS2 perfusion chamber (Bioptechs, Butler, PA) combined with an objective heater (Bioptechs) on the stage a Zeiss Axiovert 200 microscope (Thornwood, NY). Observation was using a 40× 1.0 NA oil-immersion objective lens, and fluorescence and phase contrast images were gathered using a Hamamatsu ORCA-ER charged coupled device camera (Bridgewater, NJ) driven by Openlab software (Improvision, Coventry, United Kingdom). Movies were assembled using ImageJ software.

In Vitro Assay of Interaction of Purified MyoVa C-Terminus Tail and Mlph

MBP-tagged MyoVaMSGTA and GST-tagged Mlph proteins were expressed in BL21-codon plus (DE3)-RIPL strain and purified from bacterial lysate using affinity chromatography as outlined in the manufacturer's instructions (New England Biolabs and Amersham, Amersham, Buckinghamshire, United Kingdom, respectively). GST-Mlph, 100 pmol, was mixed with 100 pmol MBP-MSGTA in buffer A (50 mM Tris-HCl, pH 7.5, 150 mM NaCl, 5 mM $MgCl_2$, 1 mM DTT, and 0.075 mM Nonidet P-40) and incubated for 30 min at RT with gentle agitation. Equilibrated glutathione-Sepharose beads, 20 μl, were added to each reaction and incubated for 30 min at RT with gentle agitation. The glutathione-Sepharose beads were precipitated by centrifugation and washed twice with 1 ml buffer A. Bound proteins were eluted by boiling the beads in SDS loading buffer, and the eluates were analyzed by immunoblotting using antibodies specific for GST and MBP. Signals were analyzed using a Fujifilm LAS3000 (Tokyo, Japan) and quantified using Aida software (Aquasan, Alpharetta, GA).

Mlph Adenovirus Production, Infection of melan-ln Melanocytes and Immunoprecipitation of Overexpressed Mlph

We modified the BLOCK-iT RNA interference (RNAi) adenoviral expression system (Invitrogen) to produce replication incompetent adenoviruses that allow transient expression of Mlph proteins in melan-ln melanocytes. To allow insertion of the Mlph coding sequence into the adenovirus packaging vector pAd/BLOCK-iT-DEST pENTR286 was constructed on the backbone of pENTR/U6 (Invitrogen) by swapping the U6 promoter and termination signal of PolIII with the expressing cassette as follows. First, a polylinker (with BglII, EcoRI, BsiwI, SpeI, NotI, SacII, KpnI, SacI, and BamHI restriction sites) was inserted into pEGFPC2 vector (Clontech, Mountain View, CA) by annealing the appropriate primers and ligating into XhoI/BamHI sites. The EGFP coding sequence was then removed from the modified pEGFP vector by restriction digest AgeI/BglII, overhanging ends were filled-in using Klenow fragment, and the vector was religated. The expression cassette (CMV promoter/polylinker/sv40 poly adenylation signal) was amplified by PCR from the previously modified vector using Phusion DNA polymerase (New England Biolabs, Hitchin, Herts, United Kingdom). To methylate the internal XbaI site, the PCR product was cloned into pcDNA3.1/V5/His-TOPO vector (Invitrogen). The expression cassette was released from pcDNA3.1/V5/His using SalI/XbaI previously introduced by PCR and inserted into pENTR/U6 using the same restriction sites, resulting in a mammalian expression vector (pENTR286) with the CMV promoter/polylinker/SV40 polyadenylation signal flanked by attL1 and attL2 sequences. pENTR286 vectors encoding N-terminal V5-tagged Mlph1-266aa, Mlph1-400aa, Mlph1-490aa and Mlph1-590aa were prepared by PCR amplification of the appropriate fragments of Mlph using IMAGE clone 4862487 as a template. Incorporation of the CMV promoter/Mlph/sv40 polyadenylation signal cassette into the adenovirus packaging vector was performed using LR clonase II (Invitrogen) to allow site-specific recombination between pENTR286 attL sites and pAd/BLOCK-iT-DEST attR sites. Pac1-digested recombinant packaging vector was then transfected into a producer cell line HEK293A, and recombinant viral particles were harvested after lysis of infected cells 14 d later. Multiplicity of infection (MOI) of viral preparations was determined by infection of confluent monolayers of HEK293A cells with serial diluted viral lysates, followed by quantification of viral plaque formation 6 d later. Infection of melanocytes at a MOI of 10^4 virus particles/melanocyte resulted in expression of Mlph in almost 100% of infected melanocytes 24 h later, as determined using immunofluorescence microscopy (unpublished data). For immunoprecipitation of V5-Mlph, 10^6 melan-ln cells were infected with V5-Mlph expressing adenovirus for 24 h. Cells were then lysed into buffer (20 mM Tris, pH 7.5, 150 mM NaCl, 1 mM DTT, 1% CHAPS, and 1× protease inhibitor cocktail). Postnuclear supernatant (PNS) was then incubated with 2 μg of mouse anti-V5 and 50 μl of sheep anti-mouse Dynabeads (Dynal, Invitrogen, Paisley, United Kingdom) overnight at 4°C with end-over-end rotation. Immune complexes were then harvested using the Dynal magnetic particle collector, washed three times using buffer, subjected to SDS-PAGE, and immunoblotted using rabbit antibodies specific for V5 and MyoVa as described below.

Immunoblotting

Cells were lysed by resuspension in buffer (20 mM Tris, pH 7.5, 100 mM NaCl, 1 mM DTT, 0.1% CHAPS, and protease inhibitor cocktail) followed by sonication. PNS was prepared by centrifugation at 1000 × *g* for 15 min at 4°C, resolved using 10% SDS-PAGE, and transferred to PVDF membranes. Membranes were blocked in solution 2 (PBS, 0.2% Tween-20, 5% nonfat dry milk), incubated with primary antibody diluted in solution 3 (PBS, 0.2% Tween-20) for 1 h to overnight, and washed with solution 3, followed by incubation for 30 min with 1:10,000 dilution of appropriate HRP-conjugated secondary antibody (Dako, High Wycombe, Bucks, United Kingdom) diluted in solution 2 and washing as before. Bound antibody was detected using the ECL Substrates (Amersham). Blots were calibrated with prestained molecular weight standards (Bio-Rad, Hemel Hempstead, Herts, United Kingdom). Conditions for 4B12 mouse anti-Rab27a and DB51 rabbit anti-MyoVa have been described previously (Hume *et al.*, 2002), and goat anti-Mlph (Everest Biotech, Oxford, United Kingdom) was used at 0.5 μg/ml.

RESULTS

Immortal melan-ln Cells Appear Indistinguishable from Primary ln/ln Melanocytes

To establish a cell culture melanosome transport assay with which to examine the role of different domains of Mlph and its binding partners in melanosome transport in living melanocytes, we generated immortal *ln/ln* melanocyte cell lines derived from mice doubly homozygous for the *ln* and *ink4A* null alleles, as described previously for an *ashen* cell line (see details in *Materials and Methods*; Ali *et al.*, 2004). These cells can be transfected and microinjected, allowing overexpression of wild-type and mutated Mlph molecules. In all aspects tested, melan-ln cells appear identical to *ln/ln* primary cultured melanocytes. First, immunoblotting and immunofluorescence microscopy of melan-ln melanocytes with antibodies specific for Rab27a, Mlph, and MyoVa proteins indicate that these cells express normal levels of Rab27a, lack detectable Mlph expression, and have a re-

Figure 2 (cont). in a typical population of transfected cells and the level of rescue of melanosome transport defects in each cell (as described in *Materials and Methods*). ■ and □, cells expressing wild-type Mlph or nonfunctional mutant Mlph, respectively. Bar, 20 μm.

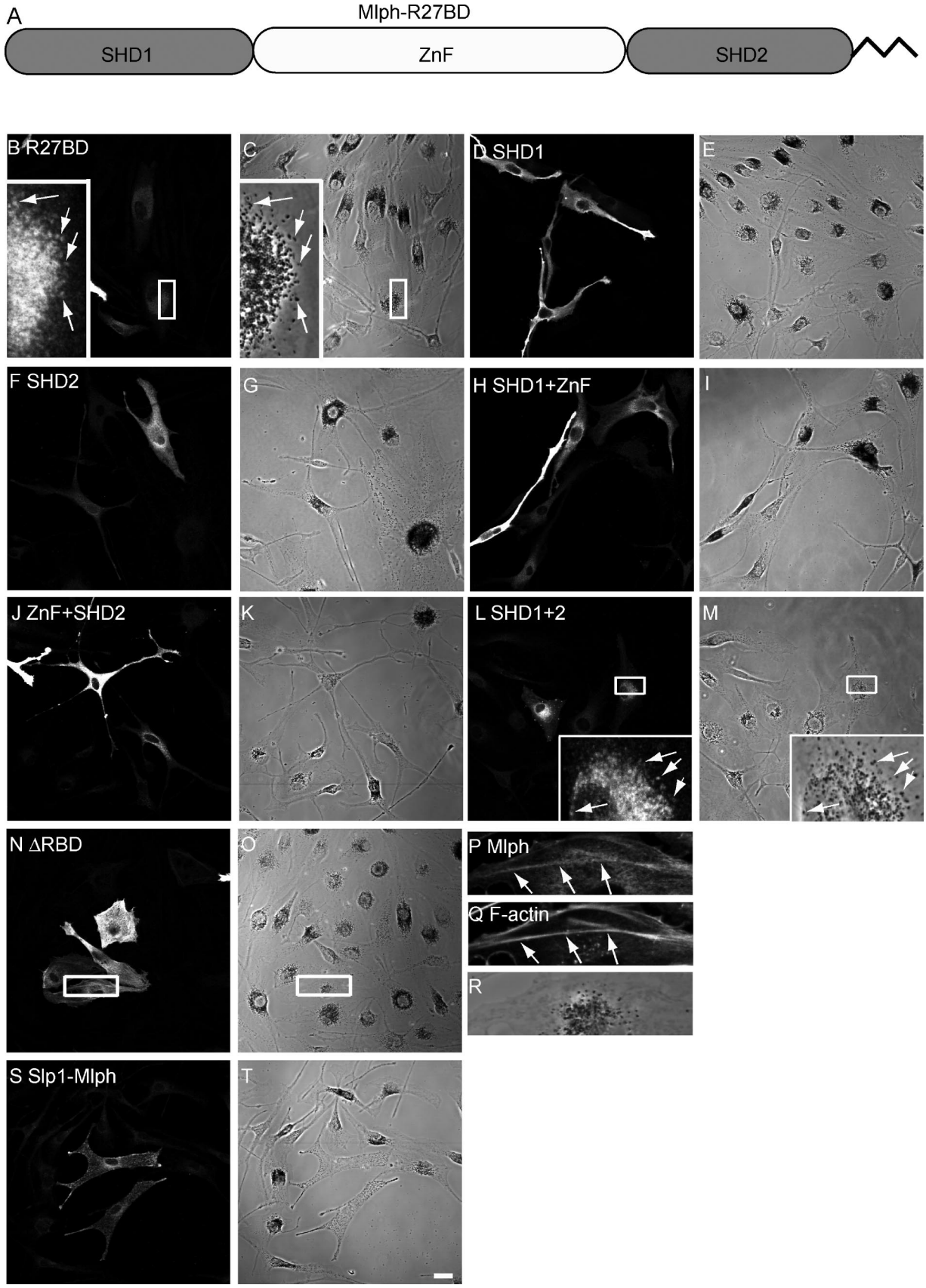

Figure 3. Both N-terminus SHD regions but not the ZnF are essential for melanosome association of Mlph. Melan-ln melanocytes were transfected with plasmids encoding myc-tagged fragments of Mlph, fixed 48 h later, and stained with antibodies (as described in *Materials and Methods*). (A) A schematic representation of the subdomains of the N-terminus R27BD of Mlph. (B, D, F, H, J, L, N, P, and S) The

duced level of MyoVa (total and melanosome-associated) relative to control melan-ink4a melanocytes (Supplementary Figure 1, A–C). Second, all immortal melan-ln cell lines exhibit perinuclear clustering of melanosomes, with the majority of melanosomes occupying only 25–30% of the total cell area, compared with cells expressing modest levels of Mlph in which typically 75–100% of the total cell area is occupied by melanosomes (Supplementary Figure 1, G and I). Immunofluorescence data confirm these observations and consistent with previous analysis of *ln/ln* primary cultured melanocytes show that Rab27a associates with melanosomes, Mlph is absent, and MyoVa is present in a diffuse pattern throughout the cytoplasm (Supplementary Figure 1, D–I, and Figure 4, A–D; Hume *et al.,* 2002; Provance *et al.,* 2002; Wu *et al.,* 2002b). Finally, many of the results presented below are consistent with those obtained from initial studies conducted with primary cultures of *ln/ln* melanocytes (our unpublished observations).

We first overexpressed Myc- or EGFP-tagged Mlph fusion proteins, which results in their recruitment to melanosomal membranes, and the redistribution of melanosomes to peripheral dendrites via recruitment of MyoVa to the melanosomal membrane (Figure 2, G and H, and Supplementary Figure 1, D–G). In the course of these experiments, we observed that there is considerable variability in the length of time (from 6 to 48 h) required for overexpression of Mlph to rescue defects of melanosome transport in melan-ln melanocytes. This is illustrated in the time course of rescue shown in Figure 2, A–F. In this example, only three of four melan-ln melanocytes microinjected with a plasmid encoding EGFP-Mlph are observed to undergo rescue in melanosomes transport within the 6 h and 45 min during which this time-lapse sequence was recorded. We observed that the level of overexpression of Myc- or EGFP-tagged Mlph correlated inversely with the extent of rescue of peripheral capture of melanosomes in cells expressing levels of Mlph detectable by immunofluorescence microscopy (Figure 2, G–I). This is consistent with published observations that Mlph contains PEST sequences and is highly susceptible to degradation by cytosolic proteases and that high levels of overexpression of EGFP-Mlph in wild-type melanocytes disrupt peripheral tethering of melanosomes, suggesting that in vivo the expression level and rate of turnover of Mlph is tightly controlled (Fukuda and Itoh, 2004). Remarkably, in many instances full rescue of melanosome transport is observed in cells expressing levels of EGFP-Mlph that can only be detected using Mlph-specific antibodies to stain transfected cells (unpublished observations). Therefore, in further experiments we used an Myc-tagged Mlph fusion protein comprising six consecutive copies of the Myc epitope fused to the N-terminus of murine Mlph because this allowed us to detect lower levels of overexpressed protein than could be observed using EGFP fluorescence as a marker of Mlph expression.

SHD1 and SHD2 Are Both Required for Recruitment of Mlph to Melanosomal Membranes

We first examined the regions of Mlph responsible for its recruitment to melanosomal membranes to examine its requirements for interaction with activated Rab27a in the context of living melanocytes. Previous studies indicated that the N-terminal region of Mlph, aa 1–150 in mouse, which contains SHD1 and SHD2, conserved in many Rab27 effectors, and an intervening ZnF, is responsible for interaction with Rab27a and has been termed R27BD (Rab27a binding domain; Fukuda, 2002; Fukuda *et al.,* 2002; Strom *et al.,* 2002; Wu *et al.,* 2002a). Within this region, SHD1 is proposed to be sufficient for interaction with GTP-bound Rab27a in vitro (Fukuda, 2002; Strom *et al.,* 2002). We introduced several constructs encoding these domains alone or in combination into melan-ln melanocytes and determined their intracellular localization using confocal microscopy (Figure 3). We observed that only proteins containing both SHD1 and SHD2, regardless of the presence of the ZnF, are able to associate with the cytoplasmic face of the melanosome membrane (Figure 3, B, C, L, and M). All other combinations of SHD and ZnF result in proteins that are diffusely distributed throughout the cytoplasm, regardless of expression level (Figure 3, D–K, and summarized Figure 1). Conversely, a truncation mutant lacking the entire N-terminus R27BD of Mlph (MlphΔRBD) is unable to be recruited to melanosomes and instead exhibits a striated pattern of distribution, suggesting that it associated with filamentous actin (Figure 3, N and O). This was confirmed by staining transfected cells with TR-phalloidin (Figure 3, P–R). To confirm the finding that the ZnF is not required for melanosome association of Mlph, we overexpressed a chimeric construct comprising the N-terminal R27BD of Slp1 (1-116 aa; which naturally lacks the ZnF) fused to the medial and C terminal regions of Mlph (150-590 aa). We found that the chimeric protein associates with melanosomes and rescues melanosome transport, suggesting that loss of the ZnF does not significantly affect Mlph activity (Figure 3, S and T). These data indicate that both SHD1 and 2, but not the ZnF, are necessary and sufficient for association of Mlph with melanosomes, most likely via recruitment by melanosomal GTP-Rab27a.

The Role of the Medial MBD of Mlph in Recruitment of MyoVa to the Melanosome Membrane

Next, we used the melan-ln cells to investigate the regions of Mlph required for recruitment of MyoVa to the cytoplasmic face of the melanosome membrane. Previous yeast two-hybrid and biochemical studies conducted using cotransfection and immunoprecipitation to assay Mlph:MyoVa interaction together with cell biological studies in which Mlph constructs were overexpressed in wild-type melan-a melanocytes indicated that the MBD of Mlph is solely required for interaction of Mlph with MyoVa (Strom *et al.,* 2002; Wu *et al.,* 2002a; Kuroda *et al.,* 2003; Fukuda and Kuroda, 2004). Moreover, these studies indicated that two binding sites exist within this region: the first, comprising aa 146-246, interacts with the globular tail of MyoVa and activate its ATPase activity (Fukuda and Kuroda, 2004; Li *et al.,* 2005), whereas the second, comprising aa 300-400, mediates interaction with the melanocyte-specific exon F of MyoVa (Strom *et al.,* 2002; Wu *et al.,* 2002a; Li *et al.,* 2005). Hereafter, these subdomains will be referred to as GTBD (for globular tail binding domain) and EFBD (for exon F binding domain), respectively. To test the contribution of the whole MBD and these subdomains in the recruitment of MyoVa to melanosomes, we constructed and expressed in melan-ln melanocytes the following Mlph constructs: Mlph lacking specifically the entire MBD (MlphΔMBD), the entire globular tail-binding region (MlphΔGTBD) and the entire MyoVa exon F–binding region (MlphΔEFBD; Figure 4). As expected, all of these truncated proteins together with wild-

Figure 3 (cont). distribution of the indicated overexpressed protein. (C, E, G, I, K, M, O, R, and T) Transmission images showing the distribution of melanosomes. (Q) The distribution of filamentous actin as detected using Texas-red phalloidin. Arrows indicate areas of colocalization of overexpressed protein with pigmented melanosomes (B, C, L, and M) or filamentous actin (P and Q). Bar, 20 μm.

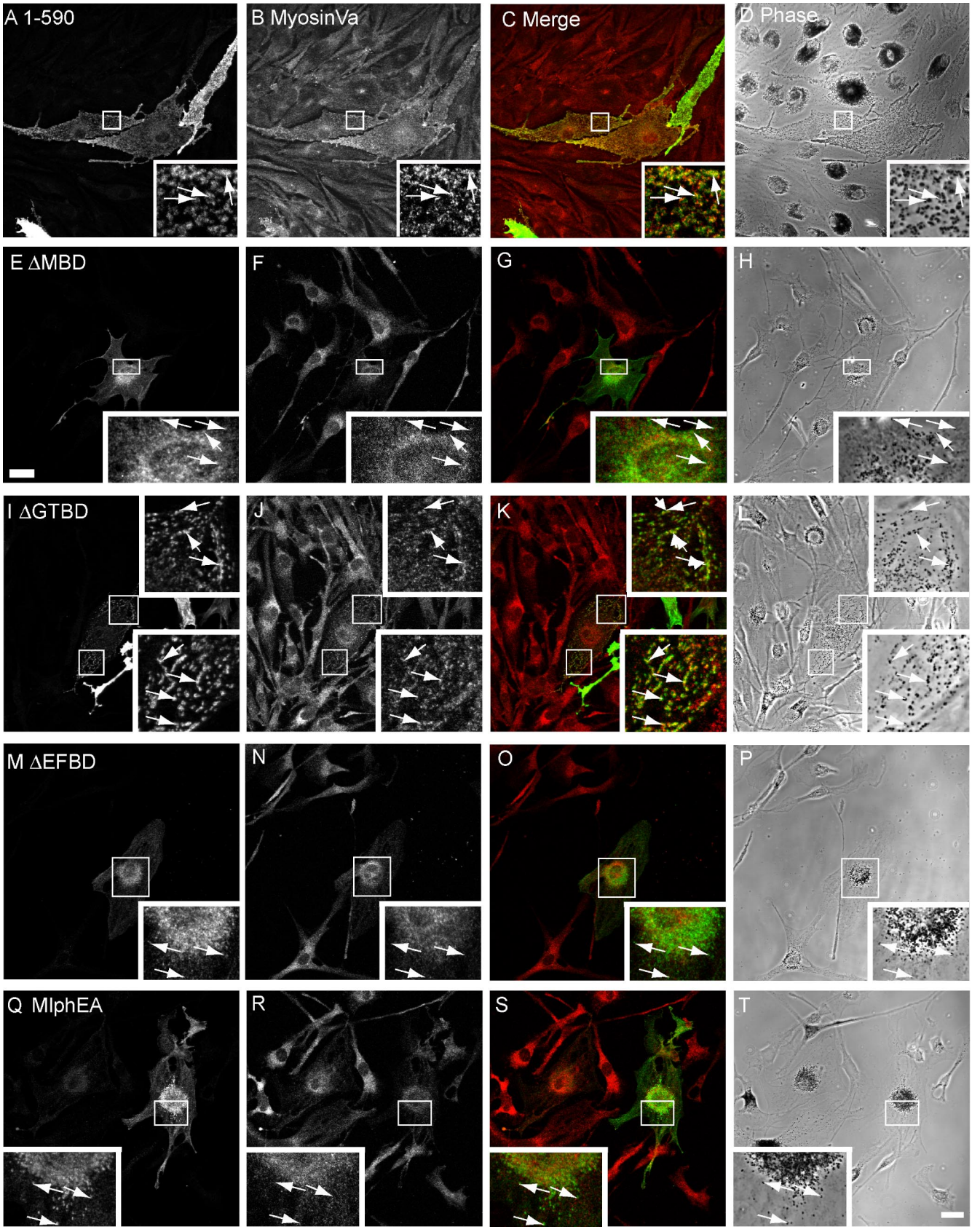

Figure 4. EFBD but not GTBD is important for Mlph mediated recruitment of MyoVa to melanosomal membranes. Melan-ln cells were transfected with plasmids encoding Mlph molecules in which the MBD is specifically disrupted, fixed 48 h later, and stained with antibodies that detect myc-tagged Mlph and MyoVa. (A, E, I, M, and Q) The distribution of the indicated overexpressed myc-tagged Mlph proteins.

type Mlph are recruited to melanosomes, indicating that integrity of the MBD is not essential for recruitment of Mlph to melanosomes (Figure 4). Consistent with published data, MlphΔMBD and MlphΔEFBD proteins are unable to recruit MyoVa to melanosomes, as determined by immunofluorescence microscopy (Figure 4, E–H and M–P). However and contrary to our expectations, MlphΔGTBD is able to recruit MyoVa to melanosomes, albeit with lower efficiency than wild-type protein (compare Figure 4, I–L and A–D, and summarized in Figure 1).

To investigate the role of the MyoVa exon F-binding region in a more specific manner, we introduced point mutations within the context of the complete Mlph protein, which replace a group of amino acids that possess acidic side chains (positions D378, E380, and E381) with alanines. This group of acidic residues is conserved between Mlph and the related protein MyRIP, and a previous study suggested that this group of charged side chains plays an important role of interaction of Mlph with MyoVa (Kuroda *et al.,* 2003). Consistent with this possibility, expression of MlphEA results in association with melanosomes but not recruitment of MyoVa to melanosomes (Figure 4, Q–T). Expression of Mlph $^{E381A/E382A}$ and Mlph^{E381A} yielded similar results (unpublished observations). These results indicate that MyoVa EFBD (300-400 aa) is necessary for melanosomal MyoVa recruitment, whereas MyoVa GTBD (150-246 aa) is not.

Identification of a Region within the C-terminus ABD of Mlph Important for Recruitment of MyoVa to Melanosomes

Having confirmed the importance of the MyoVa EFBD of Mlph in recruitment of MyoVa, we then used the melan-ln cells to test the prediction of in vitro data showing that constructs encoding the R27BD and MBD of Mlph (i.e., aa 1-400) but lacking the ABD (aa 400-590) represent the minimal fragment required for Rab27a-Mlph-MyoVa complex formation and peripheral capture of melanosomes (Fukuda *et al.,* 2002; Nagashima *et al.,* 2002; Strom *et al.,* 2002; Wu *et al.,* 2002a). To do this, we transiently overexpressed Mlph molecules truncated at the C-terminus in melan-ln and performed experiments as above. As expected from in vitro binding studies we found that, in contrast to wild-type Mlph (Figures 2 and 5, A–D, and Supplementary Figure 1), expression of the Mlph C-terminus truncated aa 266 (containing the R27BD and GTBD) results in a protein that associates with melanosomes but is unable to recruit MyoVa to melanosomes (Figure 5, E–H). Surprisingly, we found that expression of a construct encoding the intact R27BD and MBD (aa 1-400) of Mlph in melan-ln melanocytes is also unable to promote recruitment of MyoVa onto melanosomes (Figure 5, I–L). This is in spite of the fact that the construct induced production of a stable protein of the expected molecular weight (unpublished observations), which associates with melanosomes. This suggests that region(s) within the C-terminal ABD (aa 400-590) are required in situ for the association of MyoVa with melanosomal Mlph.

In search of the minimal fragment of Mlph that enables recruitment of MyoVa to melanosomes, we observed by confocal immunofluorescence microscopy that a construct encoding aa 1-483 of Mlph could recruit MyoVa to melanosomes, albeit with lower efficiency than wild-type Mlph, and that the 1-466 fragment recruited significantly less (Figure 5, compare Q–T with M–P). This finding indicates that a region within the C-terminal region of Mlph between aa 400 and 483 is required together with the N-terminal R27BD and medial MBD in order to allow recruitment of MyoVa to melanosomes and highlights the fact that the in vivo requirements are more stringent than the in vitro studies would suggest. In addition, we noticed that Mlph1–483 is able to rescue melanosome transport defects of melan-ln cells with efficiency similar to that of full-length Mlph1–590 (compare Figure 5, A–D with Q–T, and see also Figure 8B). This observation indicates that the integrity of parts of Mlph involved in interaction with actin (400-590 aa) and microtubule-associated protein EB1 (490-590 aa) are not essential for Mlph function as assayed using this method. To further test the functional importance of the interaction of Mlph with actin, we used the MlphKA mutant in which a cluster of conserved basic amino acids (K493, R495, R496, and K497 in mouse) that is reported to provide a binding site for actin are converted to alanines (Kuroda *et al.,* 2003). Consistent with the idea that the interaction of actin with Mlph is not absolutely critical for Mlph function, we observed that MlphKA is able to overcome melan-ln melanosome transport defects with similar efficiency to wild-type Mlph (Figure 5, U–X, Figure 8B, and summarized in Figure 1).

The Potential of Mlph Region 440-483 aa to Form Coiled-Coil Structure Is Essential for Melanosomal Recruitment of MyoVa

The three-dimensional structure of Mlph has yet to be solved; however, structure prediction software (such as the COILS and MultiCoils coiled-coil prediction algorithm) predicts that the aa 440-483 region of Mlph contains an amphipathic α-helix that may associate with other similar α-helices to form a coiled-coil structure (Lupas *et al.,* 1991; Lupas, 1997; Wolf *et al.,* 1997; Figure 6A). We hypothesized that formation of a coiled-coil structure in region 440-483 is important for Mlph function and decided to test this prediction using point mutations that specifically disrupt this structure within the context of the full-length protein. As with other coiled-coils, aa 440-483 region contains a heptad repeat pattern of amino acids with those at the *a* and *d* positions possessing hydrophobic side chains, whereas amino acids at positions *e* and *g* possess charged side chains (Mason and Arndt, 2004). To specifically disrupt this potential structural motif, the T residue at position 460 (corresponding to the *d* position of the heptad repeat) was replaced by P, predicted to greatly reduce the probability of coiled-coil structure in this region as determined using the MultiCoils algorithm (Figure 6A). Overexpression of Mlph^{T460P} results in a protein of the predicted size (unpublished observations), which is able to associate with melanosomes but is unable to promote the stable association of MyoVa with melanosomes (Figure 6, B–E). Similar point mutations with respect to the periodicity of the coiled-coil heptad repeat, Mlph^{M453P} (and Mlph^{A467P}; unpublished observations), yielded similar results, i.e., melanosome-associated Mlph proteins that are unable to recruit MyoVa to melanosomes (Figure 6, A and F–I). These results are entirely consistent with structure predictions. Interestingly, Mlph^{M453P} is predicted to result in a protein with a shorter coiled-coil structure (aa 454-483; Figure 6A). The latter observation suggests that the size of the potential coiled-coil structure is important.

We extended these observations by testing other Mlph mutants in which T460 is replaced with amino acids other

Figure 4 (cont). (B, F, J, N, and R) The distribution of endogenous MyoVa. (C, G, K, O, and S) Merged fluorescence images showing the extent of overlap myc-tagged Mlph (green) and MyoVa (red). (D, H, L, P, and T) The corresponding transmission images showing the distribution of pigment in transfected cells. Arrows indicate the position of myc-Mlph associated with pigmented melanosomes. Bar, 20 μm.

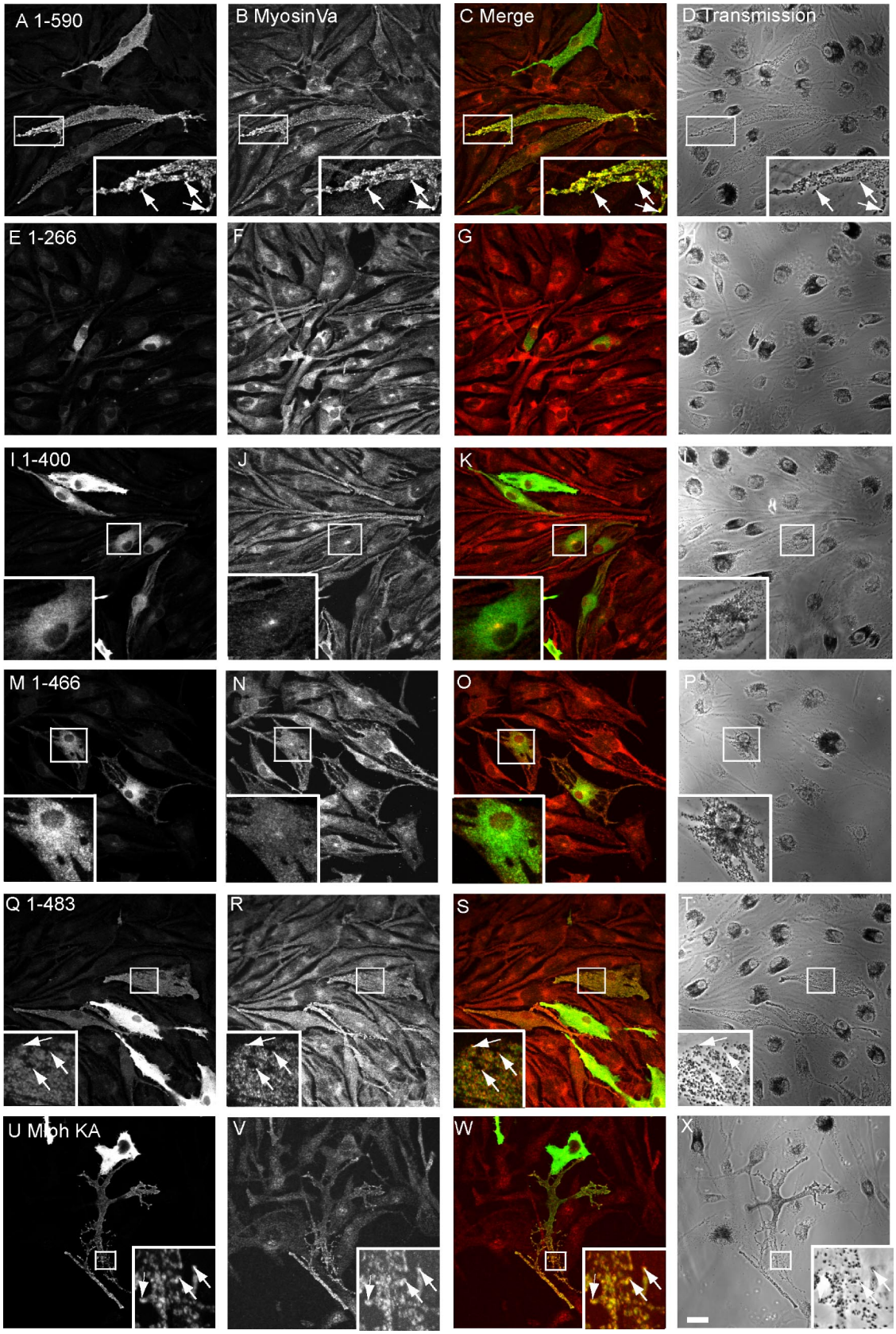

Figure 5. Rescue of melan-ln melanosome transport defects requires part of the ABD in addition to R27BD and MBD sequences. Melan-ln melanocytes were transfected with plasmids encoding the indicated C-terminus–truncated Mlph molecules, fixed 48 h later, and stained with antibodies to detect myc-tagged Mlph and MyoVa. (A, E, I, M, Q, and U) The distribution of myc-tagged Mlph molecule as indicated. (B, F, J, N, R, and V) The distribution of endogenous MyoVa. (C, G, K, O, S, and W) Merged fluorescence images showing

than P, which affect to varying extent the potential for Mlph 440-483 to form coiled-coil structure. Although P is likely to introduce a kink into the peptide backbone of the mutant Mlph and thus may have long range effects on the structure, other changes might have a more specific effect of disrupting locally the coiled-coil (Figure 6A). We observed that there is an inverse correlation between melanosomal recruitment of MyoVa by these Mlph mutants and their potential to disrupt the potential coiled-coil structure (Figure 6, A and J–Q).

Sequence comparison indicates that this region of Mlph shares high similarity at the amino acid level with the corresponding region of MyRIP, which is also predicted to form coiled-coil structure by the MultiCoils algorithm (unpublished observation; aa 724-765 in rat sequence; Figure 6A). This led us to test the possibility that this part of both proteins allows a conserved function or interaction, because MyRIP is able to bind MyoVa (Fukuda and Kuroda, 2002). We thus constructed and expressed a chimeric protein (MlphCC) in which aa 433-511 of Mlph are replaced with aa 699-782 of MyRIP (rat) in melan-ln melanocytes. As expected, this protein is localized to melanosomes and is able to promote association of MyoVa with the cytoplasmic face of melanosome membranes (Figure 6, R–U, and summarized in Figure 1). Together these data provide strong evidence that the capacity of region 440-483 to form a coiled-coil structure contributes to melanosomal recruitment of MyoVa by both Mlph and MyRIP.

The Coiled Coil Structure of Mlph Region 440-483 Enhances Mlph MBD Interaction with MyoVa

As a first step to test the mechanism by which the coiled-coil forming Mlph region amino acids 440-483 allows MyoVa recruitment to melanosomes (and rescue of melan-ln melanosome transport defects discussed below), we produced recombinant Mlph and MyoVa proteins and tested their ability to interact in vitro. To efficiently express GST-tagged Mlph protein in *E. coli*, the R27BD was omitted from all proteins because this region contributes significantly to instability of recombinant Mlph (our unpublished observations). Consistent with published data, we observed that GST-fusion proteins containing the GTBD (aa 150-266) and MBD (aa 150-400), but not GST alone or the coiled-coil region alone (Mlph aa 400-500) are able to interact with the cargo-binding tail of MyoVa aa 1258-1853 containing the melanocyte-specific exons D and F (hereafter referred to as MSGTA; Figure 7A, lanes 1-3 and 7, and 7B, lane 1; Fukuda *et al.*, 2002; Nagashima *et al.*, 2002; Strom *et al.*, 2002; Wu *et al.*, 2002a). Nevertheless, a GST-fusion protein containing the MBD together with the coiled-coil region (Mlph150-500) is able to interact significantly more strongly with MSGTA than either of these regions in isolation (Figure 7A, lane 4). Furthermore, the enhancement of interaction is ablated by the introduction of point mutation A467P (Mlph150-500AP) predicted to disrupt the coiled-coil structure of this region (Figure 7A, lane 5). These data are consistent with results observed in living cells and suggest that the coiled-coil region enhances the ability of Mlph MBD to interact with MyoVa.

However, in contrast to the results obtained from the melanosome transport assay that suggest that the GTBD fulfils a nonessential function (Figure 4), we observed that a fusion protein containing EFBD and coiled-coil regions (Mlph300-500, Figure 7A, lane 6) interacts with MSGTA to a lower extent than Mlph150-500, indicating that the GTBD contributes significantly to the ability of Mlph150-500 to interact with MSGTA. One explanation for this discrepancy between in vitro and cell culture results is that the extreme C-terminus, present in MlphΔGTBD, may compensate for the loss of GTBD in allowing sufficient MyoVa to bind to Mlph to allow rescue of melanosome transport. Accordingly, we found that Mlph300-590 is able to associate with MSGTA with efficiency similar to that of Mlph150-500, whereas a fusion protein containing the MBD, coiled-coil and extreme C-terminus region (Mlph150-590) is able to interaction with MSGTA with significantly higher affinity than that of Mlph150-500 or any of the other truncated proteins (Figure 7B, lanes 3-5). Once more results using an equivalent fusion protein in which A467 is replaced by P (Mlph150-590AP) confirm the important contribution to this interaction that is played by the coiled-coil (Figure 7B, lane 6). This mutant reduces the level of MyoVa interaction to a level below that achieved by proteins such as Mlph300-590 and Mlph150-500 that correspond to rescuing proteins in the melanosome transport assay (Mlph1-483 and MlphΔGTBD, respectively).

These observations suggest that the Mlph EFBD and coiled-coil must be present in combination with either the GTBD or the extreme C-terminus in order to allow sufficient MyoVa interaction to promote rescue of melan-ln melanosome transport defects. To further test this hypothesis in the melanosome transport assay, we expressed Mlph lacking both GTBD and the extreme C-terminus (Mlph1-483ΔGTBD) in melan-ln melanocytes. Consistent with in vitro data, we found that this protein is unable to promote rescue of melanosome transport (Figure 8B).

As a second approach to examine the role of the coiled-coil and extreme C-terminus of Mlph in MyoVa binding, we investigated the interaction of C-terminal truncated Mlph proteins with full-length, native MyoVa protein in melanocytes using an adenovirus expression system that allows efficient expression of Mlph in almost 100% of infected melan-ln cells (Figure 7C). We then immunoprecipitated Mlph (V5 tagged) and measured the amount of MyoVa associated with the overexpressed protein. Using this approach, we found that Mlph truncated at amino acid 266 or 400 are unable to interact stably with MyoVa (Figure 7C, lanes 1 and 2). Furthermore, we observed that the wild-type protein is able to recruit MyoVa with significantly greater efficiency (4–5-fold higher) than Mlph truncated at amino acid 490 (Figure 7C, lanes 3 and 4), as predicted from the experiments described above.

Altogether these biochemical data suggest that truncated Mlph proteins do not interact with MyoVa with the same efficiency as wild-type; however, those containing the two essential domains, EFBD and coiled-coil, together with either of the other regions, GTBD and extreme C-terminus, allow sufficient levels of MyoVa bind to allow functional rescue.

Melanosomal Recruitment of MyoVa by Mlph Is Essential for Peripheral Tethering of Melanosomes in Melanocytes

Another important question that may be addressed using the melan-ln melanosome transport assay is the relationship between recruitment of MyoVa to melanosomes, activation of the MyoVa, and the retention of melanosomes within the peripheral actin cytoskeleton. To answer this question, the efficiency of rescue of melan-ln melanosome transport de-

Figure 5 (cont). the overlap of myc-tagged Mlph (green) and MyoVa (red). (D, H, L, P, T, and X) The corresponding transmission images showing the distribution of pigment in transfected cells. Arrows indicate colocalization of overexpressed protein with pigmented melanosomes. Bar, 20 μm.

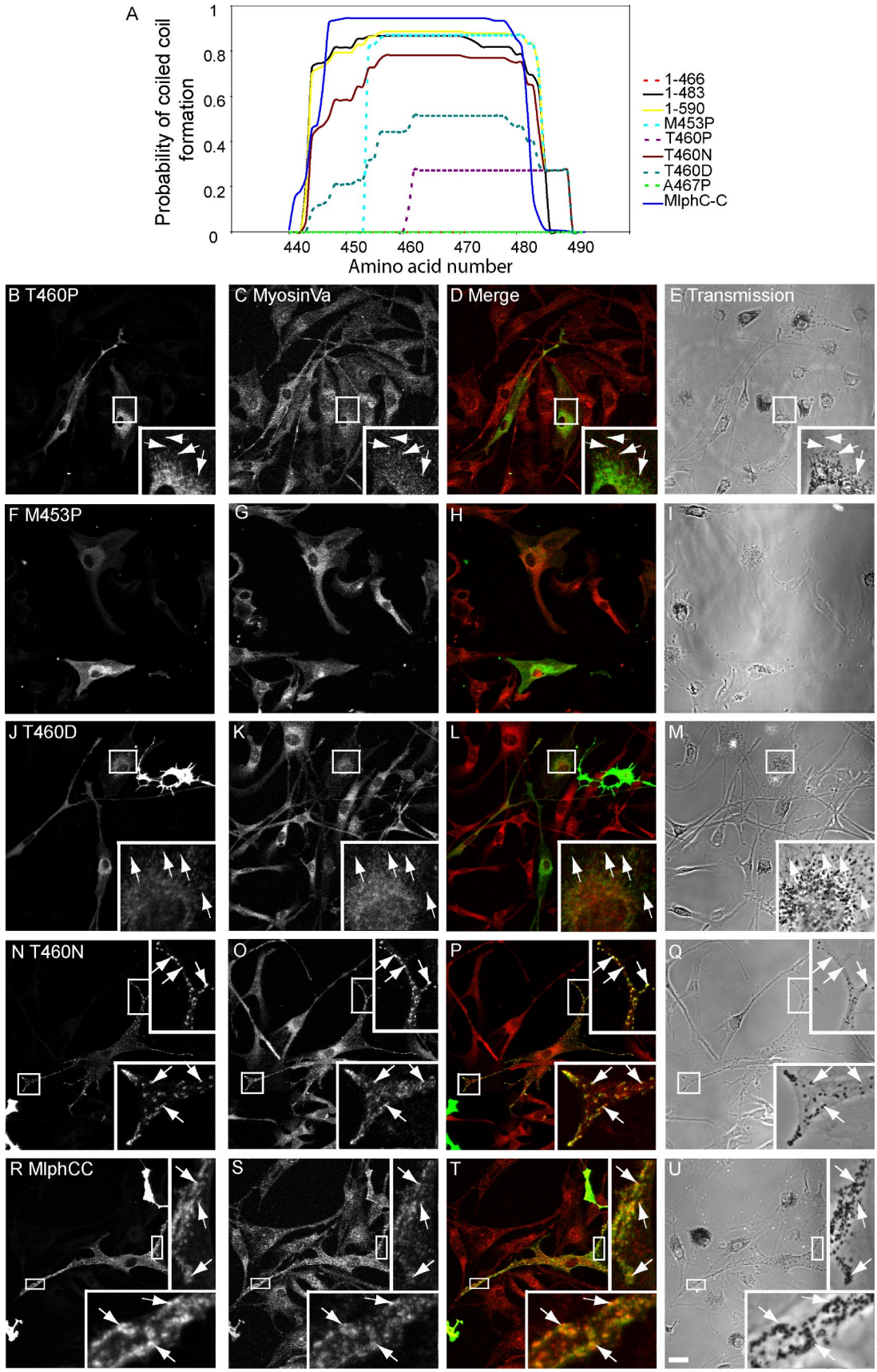

Figure 6. Mutations of Mlph that disrupt the integrity of the 440-483 coiled-coil disrupt Mlph function. (A) Prediction of coiled-coil structure in wild-type Mlph and mutant constructs correlates with rescue of melan-ln melanosome transport defects. The amino acid

fects was determined for cells overexpressing different Mlph constructs by measuring the proportion of melan-ln cytoplasm that contains melanosomes. Overexpression of wild-type Mlph resulted in rescue of melanosome transport defects, such that greater than 60% of the cytoplasmic area of melan-ln cells was filled with melanosomes, whereas overexpression of Slp1, here used as negative control, did not increase the proportion of melan-ln cytoplasm occupied by melanosomes above that of nontransfected cells (~30%; Figure 8, A–C, and unpublished data). The quantification of the ability of Mlph mutants on melanosome distribution in large populations of transfected melan-ln cells shown in Figure 8 (summarized in Figure 1; statistical significance of the results is shown in Table 1) indicates that there is a strict correlation between the ability of Mlph molecules to recruit MyoVa to melanosomes (as shown by immunofluorescence in Figures 4–6 and Supplementary Figure 1) and to promote peripheral retention of melanosomes. These data support the idea that MyoVa recruitment to melanosomal membranes is critical in allowing peripheral retention of melanosomes in melanocytes, whereas interaction with actin, MyoVa, and EB1 undertaken by the extreme C-terminus (484-590aa), and the GTBD (150-246aa) are not essential for Mlph function in this process and that the role of these pieces of Mlph is in stabilization of the core MyoVa-binding site (300-484aa).

DISCUSSION

In this study we used a cell culture melanosome transport assay to define critical functional domains of the Mlph protein. In contrast to previous studies in which overexpression of Mlph mutants was observed in wild-type melanocytes, our approach of using Mlph-null cells provides clearer information regarding the formation of the tripartite Rab27a:Mlph:MyoVa complex and in particular the contribution of Mlph domains to melanosome transport because the interpretation of results is not complicated by the presence of wild-type Mlph (Kuroda and Fukuda 2003). This system also allows the contribution of individual Mlph interacting proteins to be examined by using mutant Mlph proteins that specifically disrupt each protein:protein interaction and then assaying their function in a cellular environment.

Using the cell culture melanosome transport assay, we reached several unexpected conclusions regarding Mlph domains and interacting partners. Our data indicate that MyoVa recruitment to melanosomes and recovery of *leaden* melanosome transport defects cannot be uncoupled. Moreover, we find that a coiled-coil forming region of the Mlph C-terminus tail (aa 440-483) is essential for this function (Figures 5 and 6). Our results using the melanosome transport assay and an in vitro binding assay indicate that the coiled-coil contributes significantly to the ability of Mlph to recruit MyoVa to the melanosome membrane. This is unexpected because other in vitro studies showed that this Mlph coiled-coil region does not contribute to interaction with or activation of actin-dependent ATPase activity of MyoVa and indicated that R27BD together with MBD should allow recruitment of MyoVa to melanosomes (Nagashima *et al.*, 2002; Li *et al.*, 2005). Interestingly, it appears that the coiled-coil region alone has little affinity for MyoVa and only participates in binding when present in combination with the MBD (Figure 7). Furthermore, this coiled-coil sequence is similar to the corresponding region of the Rab27 and MyoVa/VIIa-linking protein MyRIP, and our data indicate that this region also performs the same function in activation of MyoVa (Figures 6 and 8). Although there is little primary sequence conservation between the cargo-binding tails of these different myosin motors, the conservation of the coiled-coil structure in MyRIP suggests that it may contribute to interaction with and/or activation of MyoVIIa and provide indications that a similar mechanism allows the activation of different myosin motors by cargo-specific proteins.

Leading from this, our second conclusion is that the integrity of the C-terminus ABD of Mlph and its ability to associate with actin, EB1 (and MyoVa, this study) appear to be dispensable for melanosome transport in melanocytes. Previously, Mlph aa 490-590 was suggested to form a binding site for EB1, whereas basic amino acids K493, R495, R496, and K497 allow interaction with filamentous actin (Fukuda 2002; Wu *et al.*, 2005). It is suggested that Mlph interaction with actin might enhance the processivity of the MyoVa motor activity, whereas EB1 is proposed to allow transport of Mlph to the periphery of melanocyte cytoplasm before Rab27a-Mlph-MyoVa complex formation, via transport at the + tips of growing microtubules. Our data argue that these interactions are likely to fulfill an ancillary function in melanosome transport as rescue of *leaden* melanosome transport defects occurs with efficiency similar to that of wild-type when Mlph1-483 or MlphKA are expressed (Figures 5 and 8). Alternatively, these interactions may play an important role in aspects of melanosome transport and pigmentation in vivo that may not be measured using this cell culture assay.

A third unexpected conclusion of our study is that the region of the MBD proposed to be important for interaction with the MyoVa globular tail (GTBD aa 150-266) makes a nonessential contribution to Mlph function. Evidence for this is that deletion of this region of Mlph does not affect the ability of the MlphΔGTBD mutant to rescue melanosome transport defects (Figures 4 and 8). However, these nonessential pieces of Mlph, GTBD and Mlph aa 490-590, appear to fulfill a role in stabilization of the core MyoVa-binding region (300-484 aa) because their presence enhances the level of MyoVa recruited to melanosome, and the presence of either of these pieces is essential for functional rescue of melanosome transport (Figures 4, 5, 7, and 8).

In addition to these unexpected conclusions, our assay allowed us to confirm the role of other parts of Mlph pre-

Figure 6 (cont). sequence of wild-type and mutant Mlph molecules was analyzed using the MultiCoils coiled-coil prediction algorithm available online at http://multicoil.lcs.mit.edu/cgi-bin/multicoil. The chart shows in detail the analyses of aa 440-492 of each construct as determined using the MultiCoils prediction method (results from the COILS method available at http://www.ch.embnet.org/software/COILS_form.html show similar trends; unpublished data). For the chimeric construct MlphCC coil analysis of aa 455-507 shown as ClustalW alignment of protein sequences indicate that this region of the chimeric constructs corresponds to 440-492 of wild-type Mlph. Solid lines indicate constructs that allow rescue of melan-ln melanosome transport defects, and broken lines indicate constructs that fail to do so. (B–U) melan-ln melanocytes were transfected with plasmids encoding the indicated mutant Mlph molecules. Cells were fixed 48 h later and stained with antibodies that detect overexpressed Mlph and MyoVa. Panels B, F, J, N, and R show the distribution of overexpressed Mlph; panels C, G, K, O, and S show the distribution of endogenous MyoVa; panels D, H, L, P, and T are merged images showing the extent of colocalization of myc-Mlph (green) with MyoVa (red); and panels E, I, M, Q, and U are the corresponding transmission images showing the distribution of melanosomes. Arrows indicate colocalization of overexpressed protein with pigmented melanosomes. Bar, 20 μm.

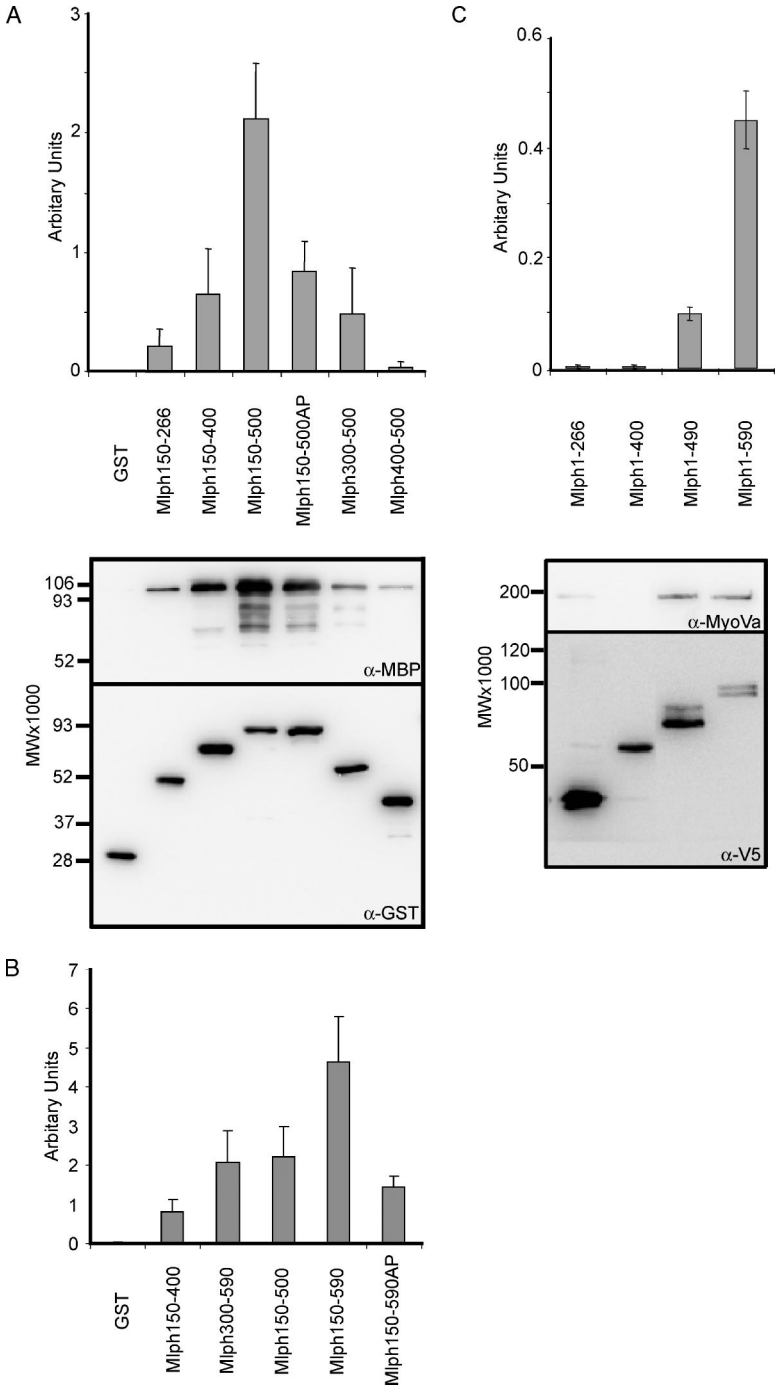

Figure 7. Measurement of the interaction of truncated Mlph proteins with MyoVa. (A and B) In vitro interaction of truncated Mlph proteins with the cargo binding C-terminus tail of MyoVa. One hundred picomoles of the indicated GST-Mlph protein was incubated with 100 pmol of MBP-MyoVaMSGTA in the presence of glutathione-Sepharose beads as described in *Materials and Methods.* Bound proteins were precipitated, eluted from the beads, and subjected to immunoblotting using α-GST and α-MBP antibodies. (C) Assay of interaction of truncated Mlph with full-length, endogenous MyoVa. melan-ln cells infected with adenovirus expressing V5-Mlph, lysed, and subjected to immunoprecipitation with anti-V5 antibodies. Immune complexes were then probed with anti-V5 and anti-MyoVa antibodies. For both assays bands (see autoradiographs in A and C) were quantified using Aida software and relative binding (see bar chart) was calculated by dividing the band intensity of MyoVa by the band intensity of Mlph. Experiments were carried out in triplicate. The migration of molecular-weight standards is indicated on the left of each blot.

dicted by earlier studies and to confirm the significance of the contribution that these parts play in Mlph function. First, we confirm that the R27BD allows association with Rab27a-GTP on melanosomes (Figure 3). Specifically we show that SHD1 and SHD2 form a minimal R27BD, whereas the ZnF is dispensable for this interaction. This is consistent with the fact that all Rab27 binding Slp and Slac2 family proteins contain SHD1 and SHD2 but not ZnF and suggests that the in situ requirements for interaction of Rab27a and Mlph are more stringent than those reported using recombinant proteins (Fukuda *et al.*, 2002). Second, our results underline the importance of the EFBD of Mlph because mutants MlphΔEFBD and MlphEA are unable to restore wild-type melanosome transport to *leaden* melanocytes (Figures 4 and 8). Thirdly, our biochemical data suggest that truncated Mlph proteins do not interact with MyoVa with the same efficiency as wild-type; however, those containing the two essential domains, EFBD and coiled-coil, together with either of the other regions, GTBD and extreme C-terminus, allow sufficient levels of MyoVa binding to allow functional rescue. This raises the possibility that there is some level of functional redundancy between the latter domains. In addition, it is possible that association of MlphMBD with MyoVa may reveal MyoVa binding site(s) within the coiled-coil and extreme C-terminus of Mlph as these regions alone (Mlph400-500 and Mlph400-590) are unable undertake inter-

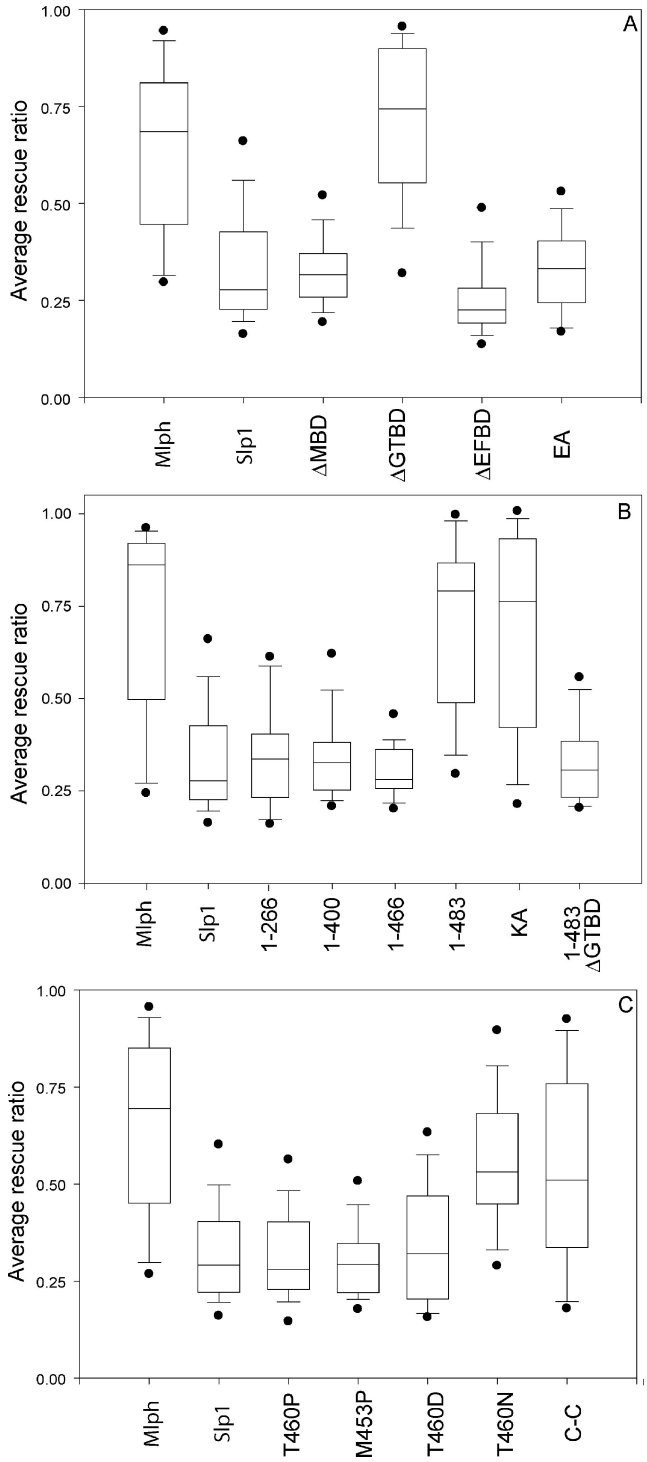

Figure 8. Quantification of the extent of rescue of melanosome transport by different Mlph mutant constructs. Melan-ln cells were transfected with the indicated constructs, and the rescue efficiency for each cell was determined as described in *Materials and Methods.* (A, B, and C) Representative results of individual experiments for constructs transfected in Figures 4, 5, and 6, respectively, together with Mlph and Slp1 controls. In all cases n = 50. Boxes indicate 25th/75th percentile, bars within boxes indicate median values, outer bars indicate 5th/95th percentile, and outer points indicate outliers.

action with MyoVa when isolated from MBD (Figure 7A; our unpublished observations).

Finally, our study addressed the relationship between recruitment of melanosomal MyoVa and recovery of melan-ln melanosome transport defects. Our finding shows conclusively that Mlph constructs that are able to recruit MyoVa (~20–40% of wild-type levels) to melanosomes also allowed melanosomes to be retained in peripheral dendrites. Melanosome transport and in vitro binding assays confirm that both EFBD and coiled-coil regions together with either GTBD or the extreme C-terminus allow this to be achieved (Figures 4, 5, and 7). This striking correlation between MyoVa recruitment and melanosome transport rescue suggests that the critical event in peripheral melanosome transport is the formation of the tripartite complex. One possibility to explain our findings is that melanosomal recruitment is somehow coupled with a conformational change in MyoVa, as has been recently proposed for its functional activation in high Ca^{2+} (Krementsov *et al.*, 2004; Li *et al.*, 2004; Wang *et al.*, 2004). Unfortunately, the activation status of MyoVa cannot be probed directly using this assay, and future studies should address this possibility using assays that measure the motor activity of MyoVa in vitro.

In conclusion, our data clearly implicate the coiled-coil region of Mlph in MyoVa binding and activation. The structural and functional conservation of this motif in MyRIP opens the possibility that a conserved mechanism for activation of MyoVa and MyoVIIa may exist. Future studies should be directed toward understanding the structural mechanism by which this is achieved.

ACKNOWLEDGMENTS

We thank Vania Braga for providing the pCS2 vector, Renato de Paulo for help with preliminary in vitro binding experiments and production of recombinant protein, other members of our lab for helpful discussions, and Lynn Lamoreux and Dot Bennett for contributions toward generating melanocyte cell lines. This work was supported by the Wellcome Trust and the Biotechnology and Biological Sciences Research Council.

REFERENCES

Ali, B. R., Wasmeier, C., Lamoreux, L., Strom, M., and Seabra, M. C. (2004). Multiple regions contribute to membrane targeting of Rab GTPases. J. Cell Sci. *117*, 6401–6412.

Bennett, D. C., and Lamoreux, M. L. (2003). The color loci of mice—a genetic century. Pigment Cell Res. *16*, 333–344.

Fukuda, M. (2002). Synaptotagmin-like protein (Slp) homology domain 1 of Slac2-a/melanophilin is a critical determinant of GTP-dependent specific binding to Rab27A. J. Biol. Chem. *277*, 40118–40124.

Fukuda, M. (2005). Versatile role of Rab27 in membrane trafficking: focus on the Rab27 effector families. J. Biochem. (Tokyo) *137*, 9–16.

Fukuda, M., and Itoh, T. (2004). Slac2-a/melanophilin contains multiple PEST-like sequences that are highly sensitive to proteolysis. J. Biol. Chem. *279*, 22314–22321.

Fukuda, M., and Kuroda, T. S. (2002). Slac2-c (synaptotagmin-like protein homologue lacking C2 domains-c), a novel linker protein that interacts with Rab27, myosin Va/VIIa, and actin. J. Biol. Chem. *277*, 43096–43103.

Fukuda, M., and Kuroda, T. S. (2004). Missense mutations in the globular tail of myosin-Va in dilute mice partially impair binding of Slac2-a/melanophilin. J. Cell Sci. *117*, 583–591.

Fukuda, M., Kuroda, T. S., and Mikoshiba, K. (2002). Slac2-a/melanophilin, the missing link between Rab27 and myosin Va: implications of a tripartite protein complex for melanosome transport. J. Biol. Chem. *277*, 12432–12436.

Hume, A. N., Collinson, L. M., Hopkins, C. R., Strom, M., Barral, D. C., Bossi, G., Griffiths, G. M., and Seabra, M. C. (2002). The leaden gene product is required with Rab27a to recruit myosin Va to melanosomes in melanocytes. Traffic *3*, 193–202.

Ito, S. (2003). The IFPCS presidential lecture: a chemist's view of melanogenesis. Pigment Cell Res. *16*, 230–236.

Krementsov, D. N., Krementsova, E. B., and Trybus, K. M. (2004). Myosin V: regulation by calcium, calmodulin, and the tail domain. J. Cell Biol. *164*, 877–886.

Kuroda, T. S., Ariga, H., and Fukuda, M. (2003). The actin-binding domain of Slac2-a/melanophilin is required for melanosome distribution in melanocytes. Mol. Cell. Biol. *23*, 5245–5255.

Li, X. D., Ikebe, R., and Ikebe, M. (2005). Activation of myosin Va function by melanophilin, a specific docking partner of myosin Va. J. Biol. Chem. *280*, 17815–17822.

Li, X. D., Mabuchi, K., Ikebe, R., and Ikebe, M. (2004). Ca^{2+}-induced activation of ATPase activity of myosin Va is accompanied with a large conformational change. Biochem. Biophys. Res. Commun. *315*, 538–545.

Lupas, A. (1997). Predicting coiled-coil regions in proteins. Curr. Opin. Struct. Biol. *7*, 388–393.

Lupas, A., Van Dyke, M., and Stock, J. (1991). Predicting coiled coils from protein sequences. Science *252*, 1162–1164.

Marks, M. S., and Seabra, M. C. (2001). The melanosome: membrane dynamics in black and white. Nat. Rev. Mol. Cell Biol. *2*, 738–748.

Mason, J. M., and Arndt, K. M. (2004). Coiled coil domains: stability, specificity, and biological implications. Chembiochemistry *5*, 170–176.

Nagashima, K., Torii, S., Yi, Z., Igarashi, M., Okamoto, K., Takeuchi, T., and Izumi, T. (2002). Melanophilin directly links Rab27a and myosin Va through its distinct coiled-coil regions. FEBS Lett. *517*, 233–238.

Provance, D. W., James, T. L., and Mercer, J. A. (2002). Melanophilin, the product of the leaden locus, is required for targeting of myosin-Va to melanosomes. Traffic *3*, 124–132.

Serrano, M., Lee, H., Chin, L., Cordon-Cardo, C., Beach, D., and DePinho, R. A. (1996). Role of the INK4a locus in tumor suppression and cell mortality. Cell *85*, 27–37.

Strom, M., Hume, A. N., Tarafder, A. K., Barkagianni, E., and Seabra, M. C. (2002). A family of Rab27-binding proteins: melanophilin links Rab27a and myosin Va function in melanosome transport. J. Biol. Chem. *277*, 25423–25430.

Sviderskaya, E. V., Hill, S. P., Evans-Whipp, T. J., Chin, L., Orlow, S. J., Easty, D. J., Cheong, S. C., Beach, D., DePinho, R. A., and Bennett, D. C. (2002). p16(Ink4a) in melanocyte senescence and differentiation. J. Natl. Cancer Inst. *94*, 446–454.

Wang, F., Thirumurugan, K., Stafford, W. F., Hammer, J. A., 3rd, Knight, P. J., and Sellers, J. R. (2004). Regulated conformation of myosin V. J. Biol. Chem. *279*, 2333–2336.

Wolf, E., Kim, P. S., and Berger, B. (1997). MultiCoil: a program for predicting two- and three-stranded coiled coils. Protein Sci. *6*, 1179–1189.

Wu, X., Bowers, B., Rao, K., Wei, Q., and Hammer, J. A., 3rd. (1998). Visualization of melanosome dynamics within wild-type and dilute melanocytes suggests a paradigm for myosin V function In vivo. J. Cell Biol. *143*, 1899–1918.

Wu, X., Wang, F., Rao, K., Sellers, J. R., and Hammer, J. A., 3rd. (2002a). Rab27a is an essential component of melanosome receptor for Myosin Va. Mol. Biol. Cell *13*, 1735–1749.

Wu, X. S., Rao, K., Zhang, H., Wang, F., Sellers, J. R., Matesic, L. E., Copeland, N. G., Jenkins, N. A., and Hammer, J. A., 3rd. (2002b). Identification of an organelle receptor for myosin-Va. Nat. Cell Biol. *4*, 271–278.

Wu, X. S., Tsan, G. L., and Hammer, J. A., 3rd. (2005). Melanophilin and myosin Va track the microtubule plus end on EB1. J. Cell Biol. *171*, 201–207.